Quantitative Kinetic Analysis by High-Resolution ^{29}Si NMR Spectroscopy of the Initial Stages in the Sol–Gel Formation of Silica Gel from Tetraethoxysilane

Colin A. Fyfe* and Patricia P. Aroca

Department of Chemistry, University of British Columbia, Vancouver, B.C., Canada, V6T 1Z1

Received December 16, 1994. Revised Manuscript Received June 9, 1995[⊗]

Silicon-29 NMR spectroscopy has been used to determine concentration time dependences of the intermediate species formed in the hydrolysis and first condensation steps in the sol–gel formation of silica gel from tetraethoxysilane. A detailed kinetic analysis of these data yields the rate constants k_1 to k_4 for the hydrolysis reactions and k_5 for the first condensation reaction. It is necessary for the fitting process to consider the last hydrolysis step as an equilibrium process, yielding k_{4f} and k_{4b}. For the first time, from measurements made at different pH values, catalyst independent rate constants have been obtained. For the hydrolysis and condensation reactions, these follow the general trend $k_1 < k_2 < k_3 > k_5$ with the associated errors reflecting the concentrations of the intermediate species.

Introduction

Silica gel is widely used as a support matrix for immobilized reagents in a variety of areas, such as catalysis, ion-exchange resins, polymer composite formulations, peptide synthesis, and in the concentration and removal of toxic materials.[1] Silica gel is often the support matrix of choice because it is an inert, nonswelling, high surface area material that is easily removed by filtration from the reaction mixture. It is surprising, considering the versatility and wide usage of this system, that in the literature there exist few quantitative kinetic analysis of the individual sequential reactions involved in the hydrolysis and condensation of tetraethoxysilane (TEOS). An important contributing factor is that the technique, namely, multinuclear NMR spectroscopy at very high fields, required to study in detail the intermediates at moderate concentrations has only recently become available.

The majority of investigations performed to date have dealt with functional group kinetic models that permit only the evaluation of global hydrolysis and condensation rate constants.[2–11] A statistical reaction model has been developed assuming that both hydrolysis and condensation reactions depend solely on the functional group reactivity and not on the local silicon environment.[10,11,17] Pouxviel and co-workers[13] have previously reported the use of high-resolution ^{29}Si solution NMR to investigate the hydrolysis of TEOS, and their results will be compared to those presented.

In the present work, high-resolution ^{29}Si solution NMR spectroscopy was used to quantitatively characterize each step of the hydrolysis and dimer formation of the acid-catalyzed homopolymerization of TEOS in water/ethanol. Rate constants as a function of the catalyst concentration (HCl) are reported, and the catalyst-independent rate constants deduced.

Experimental Section

All the samples used in this investigation were composed of the following four reagents in the quantities indicated: 1.31 M TEOS, 7.59 M ethanol, 14.5 M water acidified with HCl, and 0.0158 M of chromium acetylacetonate ($Cr(acac)_3$). At least three independent experiments were done at each pH (3.35, 3.04, 2.88, 2.76, 2.55, 2.45, and 2.33) in order to determine the pH-independent kinetic rate constants. Only pH values between 2.33 and 3.35 were studied since outside these limits the reaction proceeded either too quickly or too slowly to accurately characterize the hydrolysis and dimer formation using high-resolution ^{29}Si solution NMR spectroscopy.

A Bruker AMX 500 MHz spectrometer with a 10 mm broadband probe, maintained at a constant temperature of 300.0 ± 0.1 K, was used for the experiments. Chromium acetylacetonate ($Cr(acac)_3$) was added as a relaxation agent to reduce the ^{29}Si spin–lattice relaxation time (T_1) allowing a faster repetition time between experiments. Previous studies have shown

* To whom enquiries should be addressed.

[⊗] Abstract published in *Advance ACS Abstracts,* September 15, 1995.

(1) Brinker, C. J.; Clark, D. E.; Ulrich, D. R. *Better Ceramics Through Chemistry*; Materials Research Society Symposia Proceedings, 1984; Vol. 32.
(2) Aelion, R.; Loebel, A.; Eirich, F. *J. Am. Chem. Soc.* **1950**, *72*, 5705.
(3) Pouxviel, J. C.; Boilot, J. P.; Beloeil, J. C.; Lallemand, J. Y. *J. Non-Cryst. Solids* **1987**, *89*, 345–360.
(4) Pouxviel, J. C.; Boilot, J. P. *Mater. Res. Soc. Symp. Proc.* **1988**, *121*, 37–42.
(5) Yang, H.; Ding, Z.; Jiang, Z.; Xu, X. *J. Non-Cryst. Solids* **1989**, *112*, 449–453.
(6) Harris, M. T.; Brunson, R. R.; Byers, C. H. *J. Non-Cryst. Solids* **1990**, *121*, 397–403.
(7) Assink, R. A.; Kay, B. D. *Better Ceramics Through Chemistry*; *Mater. Res. Soc. Symp. Proc.* **1984**, *32*, 301–306.
(8) Brinker, C. J. *J. Non-Cryst. Solids* **1988**, *100*, 31.
(9) Ro, J. C.; Chung, I. J. *J. Non-Cryst. Solids* **1989**, *110*, 26.
(10) Kay, B. D.; Assink, R. A. *J. Non-Cryst. Solids* **1988**, *104*, 112–122.
(11) Assink, R. A.; Kay, B. D. *J. Non-Cryst. Solids* **1988**, *107*, 35–40.
(12) Chojnowski, J.; Cypryk, M.; Kazmierski, K.; Rozga, K. *J. Non-Cryst. Solids* **1990**, *125*, 40–49.
(13) Pouxviel, J. C.; Boilot, J. P. *J. Non-Cryst. Solids* **1987**, *94*, 374–386.
(14) Kelts, L. W., Effinger, N. J.; Melpolder, S. M. *J. Non-Cryst. Solids* **1989**, *83*, 353–374.
(15) Balfe, C. A.; Martinez, S. L. *Better Ceramics Through Chemistry II*; *Mater. Res. Soc. Symp. Proc.* **1986**, *73*, 27–33.
(16) (a) Gear, C. W. *Numerical Initial Value Problems in Ordinary Differential Equations*; Prentice-Hall: Englewood Cliffs, NJ, 1971. (b) Moore, C. *Systemized Collection of Ordinary Differential Equation Solvers*; UBC Computing Center, 1989.
(17) Assink, R. A.; Kay, B. D. *J. Non-Cryst. Solids* **1988**, *99*, 359.

0897-4756/95/2807-1800$09.00/0

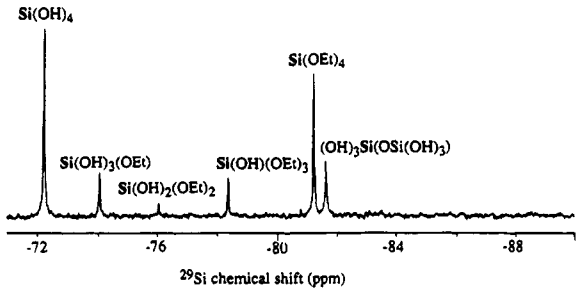

Figure 1. Typical high-resolution ^{29}Si solution NMR spectrum during the hydrolysis of tetraethoxysilane (TEOS) in water/ethanol with all the peaks assigned as indicated.

that the relaxation agent has no effect on the polymerization process itself.[14,19] T_1 measurements were performed on TEOS with different amounts of $Cr(acac)_3$ (0.000215–0.000037 mol) and the concentration 0.016 M was chosen since no significant line broadening was observed and it approaches the limit of the $Cr(acac)_3$ solubility in the solvent system. At this concentration, TEOS initially had a ^{29}Si T_1 value of 1.7 s. The ^{29}Si T_1 values of TEOS and all the hydrolyzed intermediate species were found to be very similar. Two kinetic runs were performed, one where the recycling delay was $2 \cdot T_1$ and the other where the recycling delay was $1 \cdot T_1$. The concentration profiles of all the hydrolysis species were identical for the two kinetic runs. The Ernst angle equation was therefore used to optimize the signal/noise ratio. In both of these experiments and in all of the kinetic runs, the total observed ^{29}Si signal intensity was constant to within 3%. Eight scans were accumulated for each spectrum with a repetition time of 1 s, a 60° pulse angle on the ^{29}Si channel, and gated decoupling on the ^1H channel. Previous data indicate that the negative NOE effect is negligible in this type of system.[14,15] Spectra were collected at 2 min time intervals. In all cases enough data were acquired to well characterize the growth and decay of the different intermediate hydrolysis species concentration curves. For pH values between 2.33 and 2.55 the first 40–60 min of the reaction was analyzed. For reactions with pH values greater than 2.55 the data up to 120 min was used. In all of the data used for the fittings no peaks were detected further upfield than the dimer peak in the spectra.

Results and Discussion

1. Experimental Data. A typical ^{29}Si spectrum during the hydrolysis of tetraethoxysilane (TEOS) is shown in Figure 1 with all the peaks reaching a significant concentration, i.e., greater than 3%, during the time interval studied shown and labeled in agreement with previous literature data.[18] Under the reaction conditions, the resonances of all the monomeric species are clearly separated at this magnetic field strength while those of the condensation products are not as well-resolved, limiting studies of the formation of any oligomers more complex than the dimer. A typical example of the time dependence of the spectra during the reaction is presented in Figure 2.

To obtain kinetic data, the peak areas for all species were determined by integration over fixed individual frequency ranges throughout the whole series of spectra. This was necessary due to the small shifts in the resonance frequencies as the solvent composition changed. These integration values were reexpressed as percentages of the total concentration. The initial spectrum in all cases contained solely hydrolysis products and its total area for the ^{29}Si peaks was taken to

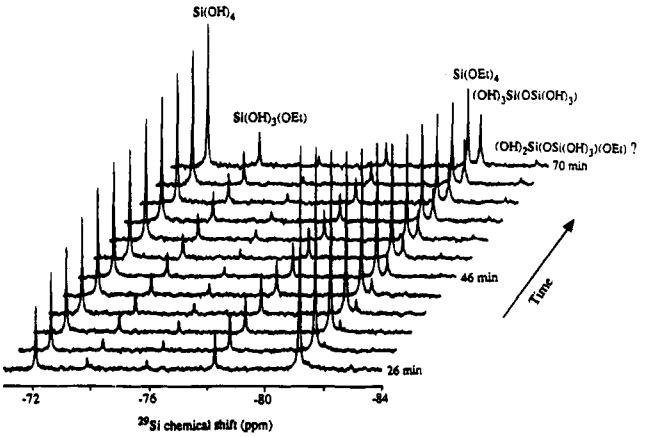

Figure 2. Time dependence of the 1D high-resolution ^{29}Si solution NMR spectra during the polymerization of TEOS at pH = 2.55.

be 100%. The percent concentration versus time graphs for all the intermediate species are shown in Figure 3 for one particular experiment (pH = 2.55) and are typical of those found at other pH values.

2. Kinetic Analysis. The simplest model that can be employed for the study of the initial polymerization of TEOS involves a series of sequential reactions that go from TEOS to the formation of the dimer. These five sequential reactions are

$$Si(OEt)_4 + H_2O \rightarrow Si(OH)(OEt)_3 + EtOH \quad (1)$$

$$Si(OH)(OEt)_3 + H_2O \rightarrow Si(OH)_2(OEt)_2 + EtOH \quad (2)$$

$$Si(OH)_2(OEt)_2 + H_2O \rightarrow Si(OH)_3(OEt) + EtOH \quad (3)$$

$$Si(OH)_3(OEt) + H_2O \rightarrow Si(OH)_4 + EtOH \quad (4)$$

$$Si(OH)_4 + Si(OH)_4 \rightarrow (OH)_3Si(OSi(OH)_3) + H_2O \quad (5)$$

where $OEt = OCH_2CH_3$.

The concentrations of the intermediate species as functions of time are shown in Figure 3. It should be noted that there is a clean separation of the hydrolysis and condensation reactions under the conditions chosen justifying the kinetic analysis used. For example, at pH = 2.55, the first indications of condensed species (dimers) in the spectra occur around 30 min and after 40 min, less than 10% conversion has occurred. The separation is even clearer at higher pH values.

The TEOS intermediate hydrolysis species kinetic curves were fitted sequentially over a four-stage process which will be outlined below. Successive stages involved the controlled introduction of additional variables necessary to improve the fit. The initial step in this analysis is to make the general assumption that the overall process can be completely represented by reactions 1–4 and the effect of other "side reactions" can be neglected. Inspection of the concentration versus time curves such as those in Figure 3 reveals that the intermediate species $Si(OH)_2(OEt)_2$ and $Si(OH)_3(OEt)$ never reach concentrations greater than 10%. In fact, the $Si(OH)_2(OEt)_2$ maximum concentration is never greater than 3%. This limits the accuracy with which the rate constants can be determined using the data of these low concentration species. Fortunately, each

(18) Harris, R. K.; Knight, C. T. G. *J. Chem. Soc., Chem. Commun.* **1980**, *421*, 726.

kinetic constant is obtained by analyzing both the decay of the reactant and the growth of the product concentration.

If the water concentration is assumed to be constant (w_t = $[H_2O]_0$ = initial concentration of water), if condensation is ignored, and if back reactions are negligible, then explicit expressions (eqs 11−14) for each monomeric species can be obtained upon integration of the derivatives (eqs 6−9).

$$d[TEOS]/dt = -k_1[TEOS]_t w_t \quad (6)$$

$$d[Si(OH)(OEt)_3]/dt = (k_1[TEOS]_t - k_2[Si(OH)(OEt)_3]_t)w_t \quad (7)$$

$$d[Si(OH)_2(OEt)_2]dt = (k_2[Si(OH)(OEt)_3]_t - k_3[Si(OH)_2(OEt)_2]_t)w_t \quad (8)$$

$$d[Si(OH)_3(OEt)]/dt = (k_3[Si(OH)_2(OEt)_2]_t - k_4[Si(OH)_3(OEt)]_t)w_t \quad (9)$$

$$d[Si(OH)_4]/dt = (k_4[Si(OH)_3]_t)w_t - k_5[Si(OH)_4]_t^2 \quad (10)$$

Therefore the first step in the fitting procedure involved a nonlinear least-squares fit of eqs 11−14 considering only the first four kinetic reactions 1−4 as forward reactions. The first analysis of the data provided first approximations for the kinetic constants which were used as the starting parameters for the next step. Figure 4 presents the experimental and calculated curves from this process for pH = 2.55. To minimize the errors in the assumptions made in this approach, large water/silane and ethanol/silane ratios, 11.05 and 5.8, respectively, were chosen for the reaction mixture.

$$[TEOS]_t/[TEOS]_0 = e^{-k_1[H_2O]_0 t} \quad (11)$$

$$\frac{[Si(OH)(OEt)_3]_1}{[TEOS]_0} = \frac{k_1}{k_2 - k_1}(e^{-k_1[H_2O]_0 t} - e^{-k_2[H_2O]_0 t}) \quad (12)$$

$$\frac{[Si(OH)_2(OEt)_2]_t}{[TEOS]_0} = \frac{k_1 k_2}{k_2 - k_1}\left(\frac{e^{-k_1[H_2O]_0 t}}{k_3 - k_1} - \frac{e^{-k_2[H_2O]_0 t}}{k_3 - k_2} + \left(\frac{1}{k_3 - k_2} - \frac{1}{k_3 - k_1}\right)e^{-k_3[H_2O]_0 t}\right) \quad (13)$$

$$\frac{[Si(OH)_3(OEt)]_t}{[TEOS]_0} = \frac{k_1 k_2 k_3}{k_2 - k_1}\left(\frac{e^{-k_1[H_2O]_0 t}}{(k_3 - k_1)(k_4 - k_1)} - \frac{e^{-k_2[H_2O]_0 t}}{(k_3 - k_2)(k_4 - k_2)} + \left(\frac{1}{(k_3 - k_2)(k_4 - k_3)} - \frac{1}{(k_3 - k_1)(k_4 - k_3)}\right)e^{-k_3[H_2O]_0 t} + \left(\frac{\left(\frac{1}{k_4 - k_3} - \frac{1}{k_4 - k_1}\right)}{k_3 - k_1} + \frac{\left(\frac{1}{k_4 - k_2} - \frac{1}{k_4 - k_3}\right)}{k_3 - k_2}\right)e^{-k_4[H_2O]_0 t}\right) \quad (14)$$

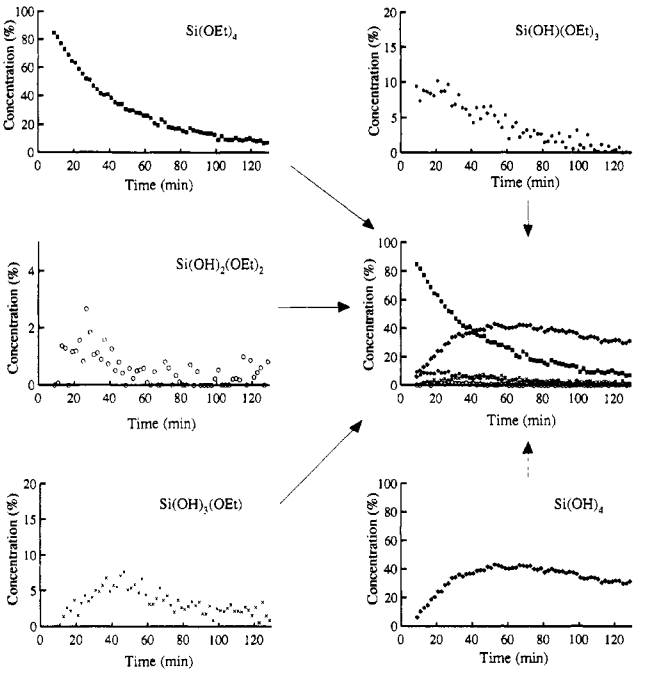

Figure 3. Time dependence of the percent concentrations of all of the intermediate species involved in the hydrolysis of TEOS as indicated, pH = 2.55.

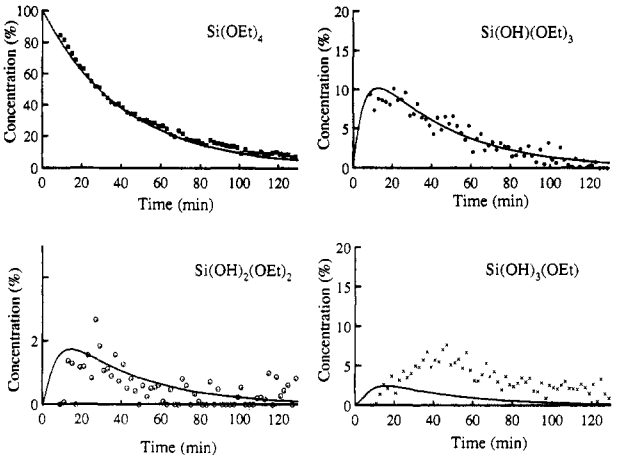

Figure 4. Calculated curves from the least-squares fitting of eqs 11−14 for the time dependence of the concentrations of the intermediate species as indicated in the hydrolysis of TEOS assuming a constant water concentration, together with the experimental data.

These high ratios reduce the variation in both the water concentration and the solvent composition as the reaction progresses. In addition, these conditions produce a better separation between the hydrolysis and condensation reactions. This approach is limited mainly by the sensitivity of the NMR experiments.

The second step involved incorporating the change in water concentration which takes place during the reaction: w_t is now replaced by

$$w_t = [H_2O]_0 - [Si(OH)(OEt)_3]_t - 2[Si(OH)_2(OEt)_2]_t - 3[Si(OH)_3(OEt)]_t - 4[Si(OH)_4]_t \quad (15)$$

The resulting differential equations 6−9 are now not explicitly solvable, requiring that the solution be obtained numerically. A new set of subroutines was

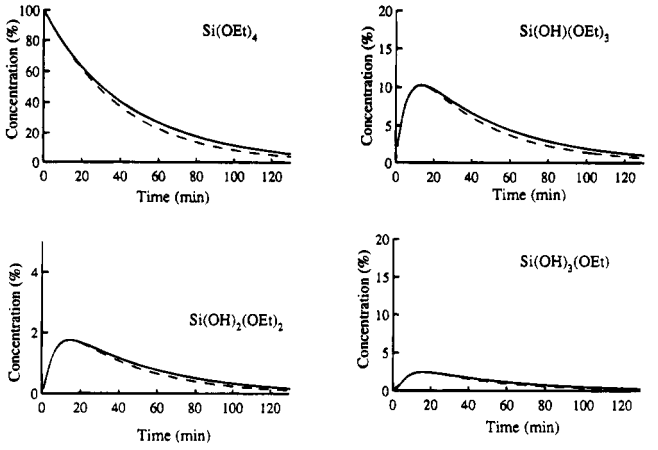

Figure 5. Comparison of different calculated curves for the TEOS system (pH = 2.55). The dashed lines are the fits obtained when the water concentration was held constant, and the solid lines are the fits taking the changes in water concentration into account.

written in order to use a program called LSODE which simultaneously integrates differential equations that are interdependent. It uses the backward differential formula approach which is a multistep method first implemented by Gear.[16] The results from the first fit were refined, and these numerical solutions were the starting points for the next step. In general, inclusion of the variation of the water concentration made little difference to the curves (Figure 5), thus it is not considered to be a critical factor in the fitting of the kinetic curves for the reactions being considered, at least under the conditions used.

The third step in the fitting procedure involved the addition of the dimer formation between two fully hydrolyzed monomers. The same methodology as described for step two was used except now eq 10 is included. By inclusion of the effect of the first condensation reaction, it was hoped that the $Si(OH)_4$ species concentration versus time curve could be properly fitted. The condensation between partially hydrolyzed species was not considered since any peaks in the region of −84 ppm, which might be indicative of $(OH)_2\mathbf{Si}(OSi(OH)_3)(OEt)$ but could also be due to a trimer species, never reached a concentration greater than the experimental scattering (3%) during the time period studied for reactions with pHs between 2.33 and 2.76. For the TEOS polymerizations taking place at pH values between 2.88 and 3.35, no partially hydrolyzed dimers were detected after 120 min.

Although the concentration of $Si(OH)_3(OEt)$ is very low, the general shape of the calculated curve does not fit the experimental data (Figure 6), yet the time dependence of the $Si(OH)_4$ product is reproduced reasonably well.

The theoretical curve of $Si(OH)_3(OEt)$ can never fit the experimental data since the model dictates that the maximum will decay to zero concentration. Experimentally, the data are characterized by a plateau after the maximum which suffers minimal decay as the reaction proceeds, suggesting that an equilibrium is established between the last and second to last intermediate species in the hydrolysis. To obtain the correct curve shape for the $Si(OH)_3(OEt)$ intermediate species, the back reaction between $Si(OH)_3(OEt)$ and $Si(OH)_4$ has to be included in the fitting procedure. This means that eqs 9 and 10

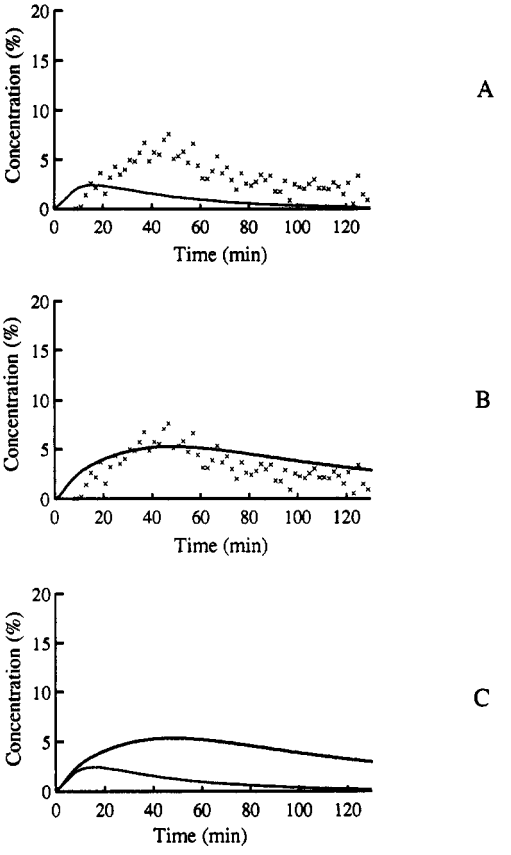

Figure 6. Comparison of the general shapes of the curves used to fit the time dependence of the concentration of $Si(OH)_3(OCH_2CH_3)$, pH = 2.55. A is the shape of the curve obtained when not considering the equilibrium back reaction. B is the shape of the curve when considering the equilibrium back reaction, and C is a comparison of these two curves without the experimental data.

must be modified to

$$d[Si(OH)_3(OEt)]/dt = (k_3[Si(OH)_2(OEt)_2]_t - k_{4f}[Si(OH)_3(OEt)]_t)w_t + k_{4b}[Si(OH)_4]_t[EtOH]_t \quad (16)$$

$$d[Si(OH)_4]/dt = k_{4f}[Si(OH)_3(OEt)]_t w_t - k_{4b}[Si(OH)_4]_t[EtOH]_t - k_5[Si(OH)_4]_t^2 \quad (17)$$

where

$$[EtOH]_t = [EtOH]_0 + [Si(OH)(OEt)_3]_t + 2[Si(OH)_2(OEt)_2]_t + 3[Si(OH)_3(OEt)]_t + 4[Si(OH)_4]_t \quad (18)$$

The new set of differential equations 6–8, 16, and 17 cannot be explicitly integrated. Consequently, these interdependent differential equations were simultaneously integrated using LSODE. It is the results from this fourth and final procedure that are presented in this paper. The effect of including this back reaction is shown in Figure 7 for reactions at pH = 2.55 together with the observed and calculated data for all the species in the hydrolysis/condensation process. It is considered that a reasonable overall fit to the data is obtained, given the complexity of the process and the simplifying assumptions made.

The final procedure was in terms of the sequential hydrolysis reactions 1–4 considering reaction 4 an equilibrium process and the first condensation step of

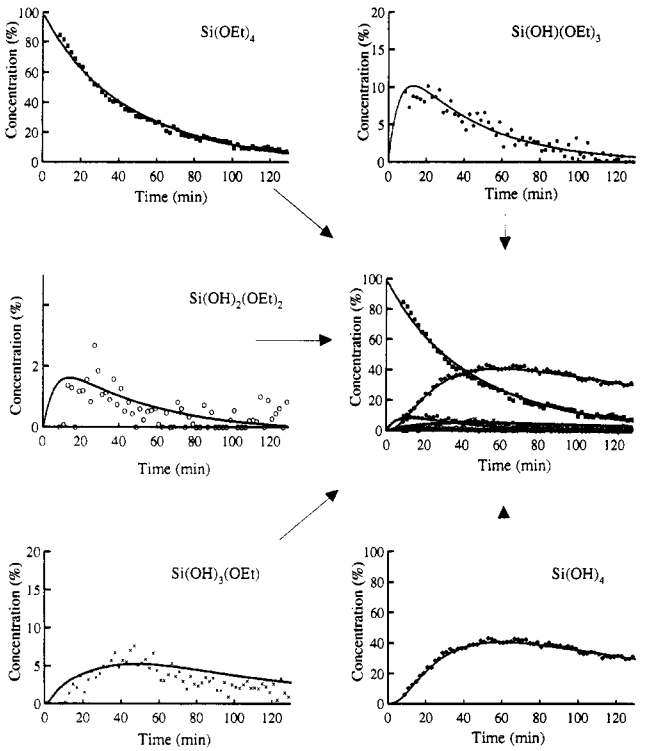

Figure 7. Time dependence of the percent concentrations of all of the intermediate species involved in the hydrolysis of TEOS together with the final calculated curves, pH = 2.55.

the completely hydrolyzed monomer, reaction 5. As will be described subsequently, experiments using ^{13}C-labeled ethanol support the decision of excluding reactions for the other hydrolysis steps.

Discussion

As previously indicated, there are some potential limitations in the model used for the fitting process in order to determine the kinetic rate constants. Only five seuqential reactions,[1-5] were taken into account with the dimer formation between fully hydrolyzed species being the only reaction depleting the monomer concentration. This is an approximation since the polymerization of TEOS could in principle involve many other reactions, some of which would directly affect the concentration of the intermediate species being considered, i.e., condensation between partially hydrolyzed species. The reaction conditions were chosen such that the majority of active hydroxyls reside in the fully hydrolyzed $Si(OH)_4$. Therefore the probability of condensation between partially hydrolyzed species is relatively low. This is supported by the fact that only for the TEOS polymerizations at pH values between 2.33 and 2.76 were signals observed that could be due to partially hydrolyzed dimers or other oligomers, and in these cases they never reached a concentration greater than 3% after 120 min. This confirms previously published data that for otherwise identical experimental conditions, alcohol-producing condensation reactions are not important in the TEOS system in contrast to the situation for tetramethoxysilane.[23]

Table 1. Average Kinetic Constants for the Hydrolysis and Condensation Steps (mol/L min) in the Reaction of TEOS (Eqs 1-5) at the pH Values Indicated[a]

pH	$k_1/10^4$	$k_2/10^4$	$k_3/10^4$	$k_{4f}/10^4$	$k_{4b}/10^4$	$k_5/10^4$
3.35	5.4 ± 0.2	36 ± 3	150 ± 50	700 ± 100	100 ± 20	120 ± 40
3.04	4.1 ± 0.8	35 ± 5	330 ± 70	830 ± 30	110 ± 50	230 ± 70
2.88	8 ± 0.1	43 ± 2	170 ± 10	600 ± 10	140 ± 10	160 ± 10
2.76	9 ± 2	70 ± 20	300 ± 100	800 ± 100	160 ± 1	200 ± 20
2.55	18 ± 1	110 ± 10	600 ± 100	500 ± 100	90 ± 30	330 ± 10
2.45	27 ± 3	140 ± 10	600 ± 100	500 ± 200	130 ± 70	400 ± 100
2.33	37 ± 1	240 ± 40	1300 ± 200	1100 ± 100	100 ± 10	600 ± 10

[a] Error estimates based on variation over the repeat experiments.

One real limitation is that two intermediate species far down the reaction chain never exceed a concentration of 10%, leading to larger errors in the fitting process of these kinetic curves and those of subsequent reactions. In addition, one of these species, $Si(OH)_2(OEt)_2$, has a curve maximum on the same order of magnitude as the estimated experimental error. To compensate, each kinetic constant can be obtained from two sets of data, the decay of the reactant and the formation of the product.

Despite these inherent limitations, reasonable fits and reliable kinetic constants were obtained. The complete set of kinetic constants determined for all pH values studied is presented in Table 1. These kinetic constants include the effect of the acid catalyst concentration. By plotting them against the acid concentration, it is possible for the first time to obtain catalyst independent rate constants for the individual reactions. Clear linear dependencies are found for four of the constants while those derived from intermediate species with small concentrations are less well defined due to larger errors (Figure 8). The final pH-independent rate constants are presented in Table 2. The data presented show the general trend for the rate constants of increasing magnitude as the number of hydroxyls increases, i.e., the hydrolysis becomes easier as n increases in $Si(OEt)_{4-n}(OH)_n$, in general agreement with previous observations.[5,12] The notable exception might be the last hydrolysis that occurs at approximately the same rate as the previous reaction; i.e., $Si(OH)_3(OEt)$ is formed almost as quickly as it is consumed. The kinetic constants also suggest that the dimer formation is slower than the formation of the fully hydrolyzed species.[20] This is confirmed by the buildup of the fully hydrolyzed species and the constant presence of a small quantity of $Si(OH)_3(OEt)$ in the reaction mixture. It is this buildup of fully hydrolyzed species that necessitates the inclusion of the equilibrum reaction for the last hydrolysis. In all the other reactions in the hydrolysis sequence, the product formed never builds up to an appreciable concentration, meaning that all other back reactions can be considered negligible when fitting the concentration curves of the different species. This approximation was checked experimentally by carrying out a duplicate reaction at pH 2.55, using ^{13}C-enriched ethanol as a solvent (>99% $HO^{13}CH_2CH_3$). In this

(19) Boonstra, A. H.; Bernards, T. N. M. *J. Non-Cryst. Solids* **1989**, *108*, 249-259.
(20) Colby, M. W.; Osaka, A.; Mackenzie, J. D. *J. Non-Cryst. Solids* **1988**, *99*, 129-139.
(21) Forsythe, G. E.; Malcolm, M. A.; Moler, C. B. *Computer Methods for Mathematical Computations*; Prentice-Hall: New York, 1977.
(22) Rosenbrock, H. H. *Comput. J.* **1960**, *3*, 175.
(23) Assink, R. A.; Kay, B. D. *Mater. Res. Soc. Symp. Proc.* **1990**, *180*, 21.

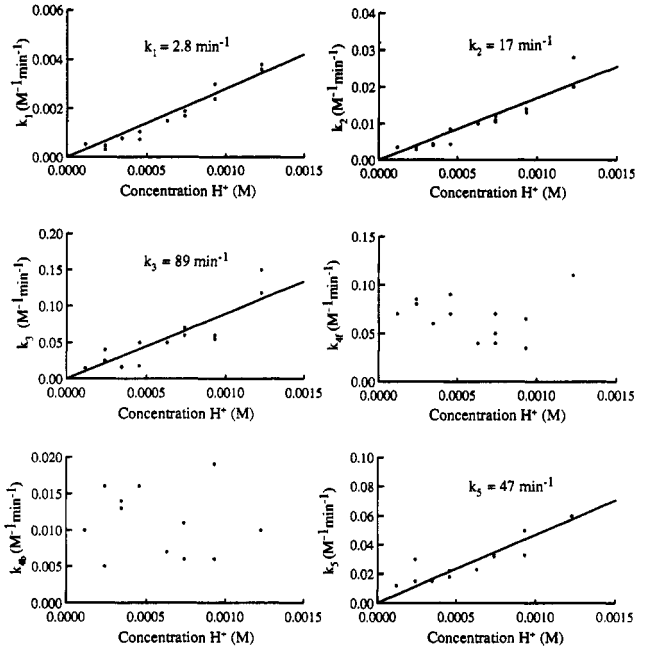

Figure 8. Plots of the kinetic constants for the different reactions as functions of pH. The lines indicated are from the least-squares fits and provide the pH-independent kinetic constants given in Table 2.

Table 2. pH-Independent Kinetic Rate Constants for the Hydrolysis and Condensation Steps in the TEOS/Water/Ethanol System (The Fits Were Constrained with the Intercept 0)[a]

kinetic rate constant	exper value (min^{-1})	corresponding reaction[b]
k_1	2.8 ± 0.1	1
k_2	17 ± 1	2
k_3	89 ± 7	3
k_5	47 ± 3	5 (dimer formation)

[a] The errors given are the standard errors of the slopes defined as

$$S_m = \sqrt{\left(\frac{\sum_{i=1}^{n}(y_i - y(x_i))^2}{n-2}\right)\left(\frac{1}{n} + \frac{\langle x\rangle^2}{\sum_{i=1}^{n}(x_i - \langle x\rangle)^2}\right)}$$

where x_i, y_i = experimental values, $y(x_i)$ = calculated value from linear regression, $\langle x\rangle$ = average value, n = number of experimental points. [b] The data for the forward and backward reactions for reaction 4 were not considered accurate enough for analysis.

situation, the contribution of $Si(OCH_2CH_3)$ groups from trans- and reesterification will be enhanced 99-fold and easily determined by ^{13}C solution NMR. By comparing the time dependences of the ^{13}C spectra for the reactions using the natural abundance and the isotopically enriched ethanol, the total number of $Si(OCH_2CH_3)$ groups reintroduced by trans- and reesterification was quantified at all stages in the kinetic process. The total number is very small, never exceeding 1% of the total number of silicon-bound ethoxy groups during the whole kinetic process. These data suggest that a very small amount of reesterification occurs, concurring with the assumption made in the kinetic model involving the lack of back reactions other than that involving $Si(OH)_4$. These observations also demonstrate that other reactions such as transesterification do not play an important role in the hydrolysis of TEOS.

It is clear from the data in Table 2 that the kinetic constants for the different reactions are neither equal nor related in some simple incremental manner as has been assumed in previous investigations. For example, Yang et al.[5] attempted to determine individual rate constants using an experimentally determined global hydrolysis rate constant and assuming relative magnitudes for the different rate constants estimated from a linear free-energy relationship. The present work shows that this is not a valid approach.

Two groups have recently determined kinetic rate constants for the individual species involved in the sequential hydrolysis and condensation reactions of two systems similar to that used in the present study.[12,13] Chojnowski et al.[12] studied the hydrolysis of TEOS in a system where dioxane was the solvent and the TEOS/water ratio was 2. The concentration dependences of the individual species were determined by quenching the reaction, trimethylsilating the intermediates at different times, and determining their relative concentrations by GC/MS. They numerically solved for the individual kinetic rate constants for this system using the Runge–Kutta–Fehlberg method[21] optimized by the Rosenbrock procedure.[22] This group obtained experimental results that differ from those presented here, when comparing values that are pH dependent. This is not unexpected given the large differences in the reaction conditions. However, a common general trend is observed, that is an increase in magnitude of the kinetic rate constants with increasing numbers of attached hydroxyl groups.

Pouxviel et al.[13] is the only other group to have experimentally obtained individual kinetic rate constants. The system studied was very similar to that presented here with respect to the individual reagent concentrations. Although they simulated their data and determined only pH-dependent kinetic constants, their results are similar to those presented in this work. In particular, the same kinetic constant ratios: k_1/k_2 and k_2/k_3 were obtained, within experimental error. Importantly, they included back reactions for all of the hydrolysis steps in order to respect the general shapes of the curves and relative positions of the maxima experimentally observed. It was only in the case of the last hydrolysis reaction that the previous workers found the reesterification reaction to make a substantial contribution to the process. This is in agreement with the results presented here. In general terms, the presented data are in good general agreement with previous results. At the present time, no literature data exist for comparison with the pH-independent rate constants which were obtained in the present work.

Conclusions

In the present work, we characterized the kinetic behavior of all the intermediate species in the sol–gel hydrolysis of TEOS by high-resolution ^{29}Si solution NMR at high magnetic field strength. As well, it was shown that it is possible to fit the quantitative kinetic data in terms of a very simple model. It is essential to include in this model the last hydrolysis step as an equilibrium reaction. From measurements made at different pH values, catalyst-independent rate constants have been obtained for the first time. These show the general trends: $k_1 < k_2 < k_3 > k_5$. Most importantly,

they clearly demonstrate that it cannot be assumed, as has been done previously, that the kinetic rate constants are the same or that there is a simple incremental relationship between them. We hope that these data will provide an unambiguous starting point for further kinetic investigations of the sol–gel process by ^{29}Si NMR spectroscopy by other workers. We are presently using them as a reference in investigations of the effect of organic drying agents and the formation of functionalized copolymer gels as well as mixed oxide functionalized systems.

Acknowledgment. The authors acknowledge the financial assistance of the NSERC of Canada in the form of Operating and Major Installation grants (C.A.F.) and the Defense Research Establishment (Pacific) (Contract W7708-0-0060). P.P.A. acknowledges the award of an NSERC Graduate Scholarship. We also thank Bruker Spectrospin (Canada) for advice and for the loan of the 10 mm broad-band probe used in these studies and Dr. D. Chong for helpful discussions on the kinetic analysis.

CM940559W